Journal of Macromolecular Science, Part A
Publication details, including instructions for authors and subscription information:
http://www.informaworld.com/smpp/title~content=t713597274

Gold Surface Adsorption Properties of the Enzymatically Polymerized Amphiphilic Decyl Ester of L-Tyrosine

Kenneth A. Marx[a]; Sam OH[a]; Anastasios P. Angelopoulos[b]
[a] Center for Intelligent Biomaterials, Department of Chemistry, University of Massachusetts, Lowell, MA [b] Chemical and Materials Engineering Department, University of Cincinnati, Cincinnati, OH

To cite this Article Marx, Kenneth A. , OH, Sam and Angelopoulos, Anastasios P.(2008) 'Gold Surface Adsorption Properties of the Enzymatically Polymerized Amphiphilic Decyl Ester of L-Tyrosine', Journal of Macromolecular Science, Part A, 45: 7, 503 — 510
To link to this Article: DOI: 10.1080/10601320802100499
URL: http://dx.doi.org/10.1080/10601320802100499

Journal of Macromolecular Science®, Part A: Pure and Applied Chemistry (2008) **45**, 503–510

ISSN: 1060-1325 print/1520-5738 online
DOI: 10.1080/10601320802100499

Gold Surface Adsorption Properties of the Enzymatically Polymerized Amphiphilic Decyl Ester of L-Tyrosine

KENNETH A. MARX,[1] SAM OH,[1] and ANASTASIOS P. ANGELOPOULOS[2]

[1]*Center for Intelligent Biomaterials, Department of Chemistry, University of Massachusetts, Lowell, MA*
[2]*Chemical and Materials Engineering Department, University of Cincinnati, Cincinnati, OH*

Received and accepted January, 2008

In aqueous solution, both amphiphilic decyl esters of the amino acids D & L-Tyrosine have been shown to self-assemble at identical low mM range c.m.c. values to form similar rod or plate-like fibers a few microns wide and with lengths ranging from tens to hundreds of microns [Mat. Sci. Eng. C11 2000 155–163]. These monomers have only slightly different rates of polymerization with horseradish peroxidase below their c.m.c. and have been shown to possess pH dependent self-assembly properties, as well as significantly increased binding to the gold surface of a quartz crystal microbalance with increasing pH [Biotech. Progress 15 1999 522–528]. In the present study, we quantitate the pH dependence and gold surface adsorption kinetics of the decyl ester of L-tyrosine using X-ray photoelectron spectroscopy (XPS) and then correlate these data with monomer solution titration studies. These data support the notion of increasing gold surface adsorption with increasing pH in the range from 5–8. We present evidence that this involves the lowered solubility of the neutral charged species resulting from the deprotonation of the α-NH_3^+ in each monomer unit. At 24 h adsorption at pH 7.0, we observed XPS evidence for complete coverage of the Au surface. From these data for the Au 4f photoelectron signal attenuation, we estimate a film thickness of 5.89 nm from the attenuation of the Au4f photoelectron intensity by the growing film.

Keywords: amphiphilic monomer; tyrosine decyl ester; pH titration; X-ray photoelectron spectroscopy; gold surface; enzymatic polymerization

1 Introduction

Horseradish peroxidase (HRP) is an enzyme that has long been used for the polymerization of a variety of monomer substrates. The enzyme possesses a wide range of substrates, is relatively stable and is commercially available (1). Phenol and its derivatives represent an important class of the most reactive substrates for HRP (2). The reactions of phenolic monomers have been studied in a variety of formats. These include organic solvents, reverse micelles, aqueous solution and at the air-water interface in Langmuir-Blodgett troughs (3–12). HRP polymerization has been shown to proceed via free radical coupling at the *ortho* or *para* ring positions for monomers in both aqueous solution and condensed states, such as the packed monolayer of the Langmuir-Blodgett trough (3, 8, 10, 13). Where the *para* position is substituted, *ortho* coupling is predominant (2).

Address correspondence to: Kenneth A. Marx, Center for Intelligent Biomaterials, Department of Chemistry, University of Massachusetts, Lowell, MA 01854. Tel.: (978) 934-3658; Fax: (978) 934-3013; E-mail: kenneth_marx@uml.edu

In traditional free radical phenolic polymerizations, interchain crosslinking is a serious practical problem. It can lead to unwanted product properties such as insolubility, heterogeneity in properties and difficulty in processing (5, 8). However, this crosslinking property is actually exploited in certain biological systems. For example, enzymatic crosslinking of phenolic polymers via the rings forms the basis for systems as diverse as tough plant cell wall structures, seed coatings and surface bioadhesive systems in marine organisms (14). However, for solution studies and systems alkyl derivatives of phenols can provide routes to self-assembly into ordered micelles, vesicles, tubules and monolayers prior to polymerization. The general characteristics of molecular self-assembly have been previously described in detail and in relation to other synthesis strategies for supramolecular structures (15, 16). Formation of well-defined supramolecular aggregates results from molecular recognition and non-covalent interaction between molecular building blocks to achieve the most thermodynamically stable state for the given system. The local order in the monomers present in these structures can aid in the synthesis of ordered product species, possessing superior processing properties (8, 10). Previously, we demonstrated that amphiphilic decyl esters of the phenolic amino acids

D & L-Tyrosine (DEDT and DELT respectively) can be polymerized by HRP in aqueous solution (11). HRP exhibits a limited stereospecificity, with the pH 6.1 optimum polymerization of the D-isomer possessing twice the rate of the L-isomer. Below 0.10 mM, both isomers exhibit a second order kinetic dependence to the overall polymerization rate (17). These isomers may also be electropolymerized on Au or Pt electrodes to form thin films that can entrap enzymes to form electrochemical biosensors (18–21).

The quartz crystal microbalance (QCM) is a useful tool for characterizing the formation and properties of thin biomacromolecule films. Previously, we have used the QCM in a novel way to investigate the pH dependent behavior of the amphiphilic DEDT monomer self-assembly followed by its polymerization with HRP (22, 23). This investigation led us to postulate the existence of self-assembled aggregates of the monomer that increased in magnitude with increasing pH over the range from 3–7. Following HRP polymerization, these aggregates possessed significantly increased viscoelastic properties (higher $\rho\eta$ product), characteristic of more energy dissipative structures, but were largely unaltered in overall shape and dimension at the resolution level of the light microscope. At the SEM level there were only minor changes evident upon polymerization by HRP (17).

In the present report, we have investigated the gold surface adsorption of HRP polymerized DELT using X-ray photoelectron spectroscopy (XPS) to characterize the change in atomic composition at the surface. The DELT adsorption was studied as a function of pH and the optimum pH identified for binding was correlated to the solution titration behavior of the monomer. We observed that polymerized DELT at the pH optimum for gold surface adsorption exhibited increasing surface coverage of the gold with complete coverage being attained at immersion times as long as 24 h. These data allowed us to estimate the average adsorbed film thickness at saturation coverage to be 5.89 nm.

2 Experimental

The DEDT and DELT monomers were prepared as described elsewhere (11). Horseradish peroxidase (Sigma Chem. Co.), hydrogen peroxide (50% solution) and methanol (Aldrich Chem.) were purchased and used as obtained. pHydrion buffers were obtained from Micro Essential Laboratory, NY. Solutions of the DEDT and DELT monomers were freshly made before each experiment. Monomers were solubilized in 1 ml of methanol to which 99 ml of deionized water was added and appropriate phosphate buffer to yield the final desired pH for the kinetics and XPS studies. At pH 6.0, the primary pH studied in these experiments, these conditions create a 100 mM phosphate buffered solution. Phosphate buffer was chosen because HRP has significant activity in this buffer system with optimum activity near pH 6.0 as previously described (11). Reactions were studied at this pH and 25°C using a Perkin-Elmer Lambda-9 UV-Vis spectrometer as previously described. The polymerization reaction, carried out at 2.5 U/ml final HRP, was initiated with the addition of H_2O_2 to a final 10 mM concentration.

XPS studies were carried out on samples at the existing pH of the solution or at an adjusted pH after addition of the appropriate small volumes of concentrated acid or base. For the XPS studies, the enzymatically polymerized samples were allowed to proceed to completion overnight, whereupon gold coated substrates were immersed in the samples for varying times at different pH values. Glass coverslips completely coated with evaporated gold were used as substrates. Following immersion in the polymerized sample solution, the gold coated substrates were carefully rinsed twice in deionized water for 3 min before being dried in a vacuum oven for 24 h. Elemental analysis by XPS was used to calculate the atomic coverage of the gold surface by the polymer. An ESCALAB MKII spectrometer with Mg$K\alpha$ radiation and a pass energy of 20 eV was used to obtain the various elemental high resolution energy spectra. A scan range of 20 eV with a minimum of 5 scans was performed to obtain each high resolution spectrum. The instrument was equipped with a constant energy hemispherical analyzer. Using adhesive backed copper tape suitable for UHV applications, the gold coated substrates were mounted on a metal pedestal in the XPS instrument. Sample surfaces were sufficiently large so that only film on the gold portion contributed to the XPS spectrum obtained. Sample surfaces were aligned perpendicular to the axis of the collecting lens. High resolution peak areas for the elements were baselined, and in conjunction with the Scofield sensitivity factors, were used to calculate atomic concentrations of the respective elements. Binding value energies were corrected to the C(1s) peak, with the adventitious C(1s) taken as 285 eV. Due to atmospheric CO_2, the gold substrates possessed substantial carbon contamination from bound CO_2 prior to immersion in the DELT solutions. Hence, adsorbate coverage on gold using Au and C atomic percentages were corrected for this contamination level.

Titration studies were performed as follows. Concentrated H_2SO_4 was added to 99 ml distilled H_2O until an initial acidic pH close to 3.0 was achieved. The monomer was then added, dissolved in 1 ml methanol. The pH was recorded and then successive additions of 50 μl of 0.02 M NaOH were carried out with pH being determined after equilibrium with mechanical stirring. The pH was measured with an Orion 920A pH meter. The moles H^+ consumed/n moles monomer quantity was then calculated from the titration data and plotted vs. pH. Since the data were not obtained in a glove box under CO_2 free conditions, equilibrium pH values could not be determined accurately in the pH range of the weak soluble CO_2/carbonate equilibrium and the data in this pH range are not shown. However, the molarity of H^+ consumed in this region is quite small with respect to the molarity of monomers being titrated and therefore, no significant fractional molar consumption of H^+ is evident compared to the monomer titration, which is dominant in the titration curve.

3 Results and Discussion

3.1 Enzymatic Polymerization of DELT

In a previous study, we examined the nearly identical self-assembly properties, HRP dependent polymerization and long fibrillar-shaped micron scale structures of both DEDT and DELT isomers (17). Also, a qualitative examination of gold surface binding was carried out using the QCM in which we observed variations in the pH dependent gold surface binding and subsequently were able to follow the polymerization of the monomers enzymatically (22). By contrast, when HRP was used to copolymerize a monomer mixture of DELT and L-tyrosineamide (1:1), and the system examined in a high resolution AFM structure study, no fibrillar structures, but an array of hemispherical structures, were observed adsorbed to gold substrates (24). In order to have greater insight into these previous results, we carried out the present study to characterize quantitatively the extent of gold binding of these amphiphilic molecules. Our aim was to quantitate the level of gold surface coverage and correlate it with the pH titration properties of the monomer functional groups. We carried out the present study using only the DELT isomer, since all of our studies have indicated no significant difference between the solution physical properties or QCM measured gold surface interaction properties of the DEDT and DELT chiral isomers.

Prior to gold binding studies, we enzymatically polymerized a 0.1 mM solution of the DELT monomer at pH 6.0. This represents a concentration below the 0.17 mM c.m.c. of DELT at this pH (17). Characteristic UV-Vis spectra at a few early time points during the HRP polymerization are shown in Figure 1. The pH 6.0 condition was chosen for display here because it represents the pH optimum for HRP activity with both the DELT and DEDT isomers (11). The DELT monomer spectrum possesses absorption peaks close to 230 nm and 270 nm. The latter peak is due to delocalized electrons in the conjugated phenol ring, the dominant side chain feature of tyrosine. With polymerization time, this absorption peak increases along with the appearance and growth of an extensive high wavelength absorption tail to the spectrum. This tail, entirely lacking in the monomer spectrum, occurs at lower intensity out to wavelengths above 600 nm and corresponds to the absorption properties of electrons delocalized in more extensively conjugated systems involving multiple ring C-C polymerization products of the HRP reaction. The Figure 1 spectrum shown for the 24 h reaction condition, represents the endpoint of polymerization, as well as the time just prior to immersion of the gold substrate for the XPS binding studies. For this condition, the long wavelength tail has reached maximum intensity relative to the unchanging monomer absorption peak intensity. These observations are consistent with completion of the polymerization reaction.

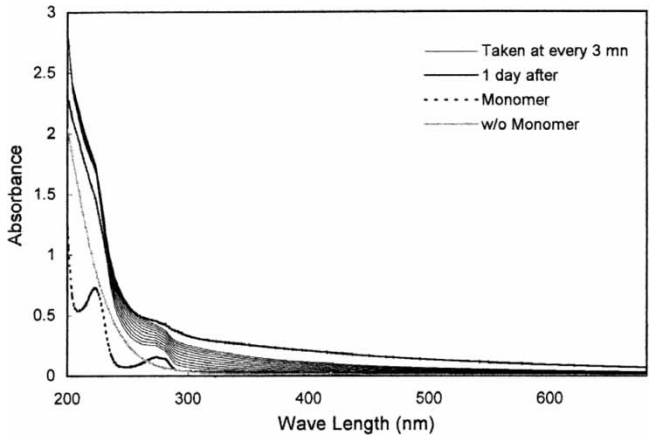

Fig. 1. UV-Visible spectra of the DELT monomer prior to polymerization and at various times during the enzymatic polymerization by HRP at 25°C and pH 6.

3.2 Gold Surface Coverage by HRP Polymerized DELT

Next, we carried out experiments adsorbing HRP polymerized DELT to gold substrates. In Figure 2, we present XPS energy spectra from the atomic orbital regions that we used to quantitate the DELT adsorption in these samples. In panel (a), the C(1s) orbital electron energy spectrum displays a characteristic single peak whose intensity was used in quantitating the total carbon percentage on the gold surface. Panel (b) shows the double peak Au(4f) orbital electron energy spectrum for an unadsorbed gold substrate. This intensity provided the percentage of unadsorbed or available gold surface. In panel (c), the N(1s) orbital electron spectrum is displayed. This directly reflects the nitrogen found in the amine group of DELT since no other nitrogen containing molecule is capable of adsorbing to the gold surface. And in panel (d), we present the Si(2p) orbital electron energy (104 eV peak) region. There is no peak at the Si(2p) energy on this or any of our adsorbed samples. This is due to the fact that the gold on our substrates, upon which adsorption occurs, completely covers the underlying glass substrates in the region of the XPS probe beam. Using the XPS spectra intensities, the % of each element observed at the surface was calculated by the XPS instrument software.

A wide variety of carbon containing compounds, including CO_2, are known to adsorb to gold surfaces. This can be observed in the data we present in Table 1 where XPS measurements are presented for a series of adsorption conditions. For all conditions, no Si% was observed, due to the complete Au film coverage of the glass slides' surfaces. A comparison of the first two data columns contrasts the elemental composition of a freshly prepared Au surface with a similar gold surface that had been washed in chloroform. There is little difference in the O% composition, due to significant and rapid CO_2 adsorption from the gas phase to the Au surface to similar extents in both cases. However, the C coverage is 30.6% greater due to chloroform adsorption, with a corresponding diminished Au coverage of nearly 30%. In the third column, we present the elemental composition of

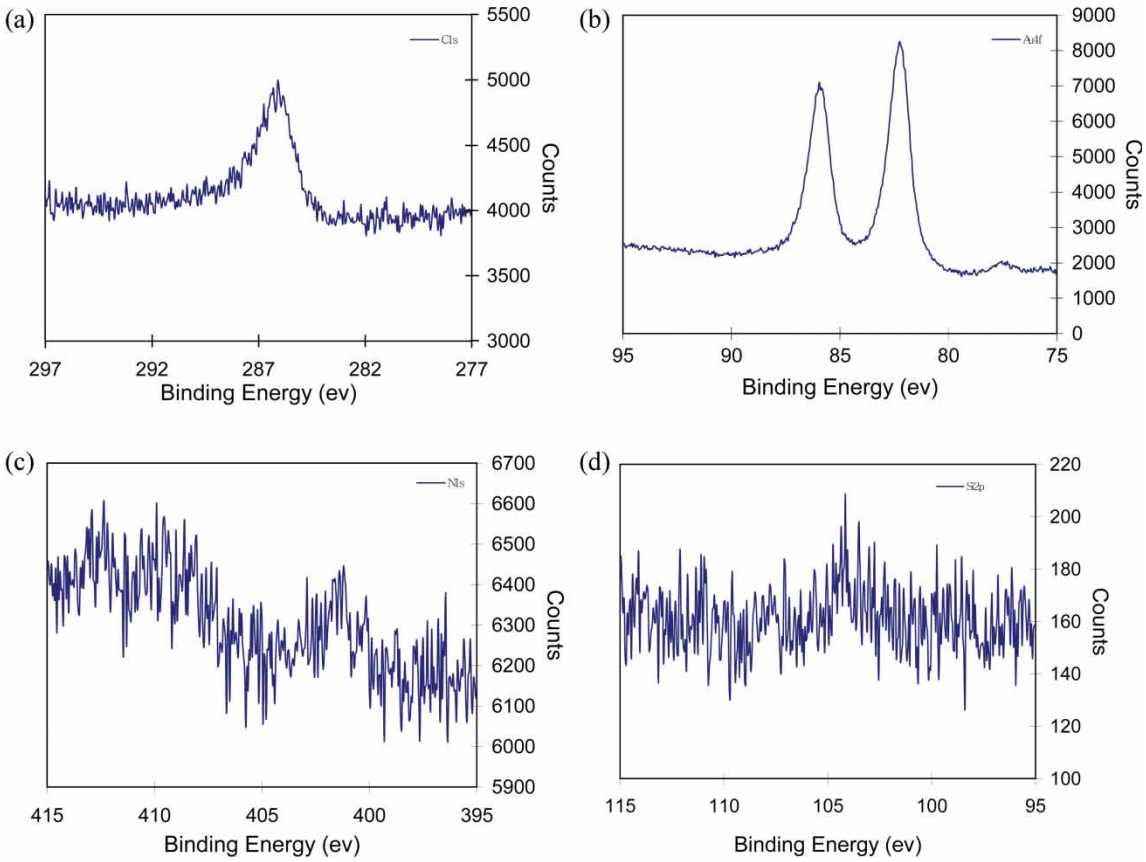

Fig. 2. Representative XPS energy spectra corresponding to the various atomic orbital electron regions we used to quantitate DELT binding to gold. (a) C(1s) orbital electron energy spectra for DELT; (b) Au(4f) orbital electron energy spectra; (c) N(1s) orbital electron energy spectra for DELT; (d) Si(2p) orbital electron energy spectra. Adsorption was for 1 h onto gold of DELT polymerized at pH 8.0 for 24 h.

the Au surface due to the DELT monomer dried directly upon the surface. Here, no Au signal was observed, indicating significant film thickness and complete surface coverage. In the case of 20 h adsorption of polymerized DELT onto Au, there remains a residual 5.3% surface Au, but the O, C and N atom composition of the surface resembles that of the dried monomer DELT film. The principal difference is that the O composition is a nearly two-fold higher%. This and the lesser C% difference for the polymerized DELT likely results from a different monomer orientation in the dried monomer film than exists for the monomers units in the adsorbed polymerized DELT.

Table 1. Atomic percentages of elements obtained from XPS analyses of various coatings on Au-coated glass substrates

	Type of coating			
Element	Bare substrate	Chloroform treated	Dried monomer	DELT polymerized at pH 6.0 for 24 h and deposited for 20 h
O	10.2	9.5	14.4	24.5
C	12.7	43.3	80.2	67.8
N	0	0	5.4	4.2
Au	77	47.2	0	5.3
Si	0	0	0	0

Next we examined adsorption of the polymerized DELT onto Au by XPS measurements in two different ways, as a function of solution pH during adsorption and as a function of time to achieve saturation coverage of the gold surface. In Figure 3, we present results for the coverage of gold by adsorption of DELT following polymerization by HRP for 24 h. This experiment was carried out in two ways. The DELT was either polymerized by HRP for 24 h at pH 6.0 or polymerized at the same pH used in the subsequent adsorption step. For the pH 6.0 polymerized sample, this was divided into samples whose pH was then adjusted to the adsorption pH prior to the adsorption step. For both HRP polymerized samples, the adsorption at the indicated pH was carried out for 1 h. At different pH values, these Figure 3 XPS data show minor differences in the level of DELT bound to gold from the two HRP polymerization protocols. At pH 6.0, as expected, the XPS coverage by polymerized DELT represented by the two C(1s) based C% values are nearly identical. This is the expected behavior since only at

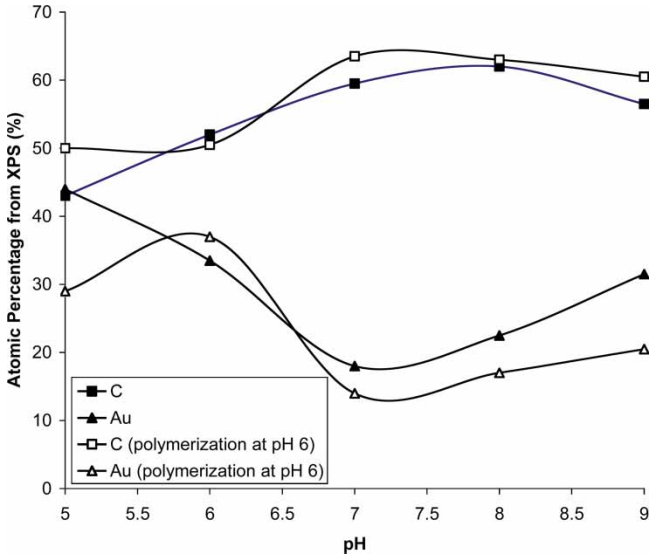

Fig. 3. XPS data for polymerized DELT adsorbed onto gold. The following two methods were used. Either: DELT was polymerized (24 h) at the indicated pH, then adsorbed onto gold during 1 h of immersion of the gold substrate (filled symbols) or DELT was polymerized (24 h) at the pH 6.0 HRP optimum, and then adsorbed at the different pH values onto gold during 1 h of immersion of the gold substrate. This data set (open symbols) is indicated in the figure as "polymerization at pH 6".

pH 6.0 are both experiments done in exactly the same fashion. At all pH values other than 6.0, there is somewhat more gold surface coverage by the pH 6.0 polymerized DELT condition. This is to be expected since the HRP rate optimum condition of pH 6.0 during the synthesis phase will create more DELT product, resulting in higher [DELT] driving net surface coverage. The effect is most pronounced at pH 5.

From both Figure 3 methodology data sets, a similar pH dependent gold binding behavior is evident. For the variable pH polymerization method, the optimum in the binding is between pH 7–8. For the pH 6.0 HRP polymerization data, the optimum pH is closer to 7.0.

3.3 Titration and Gold Adsorption Behavior of DELT and L-Tyrosine Monomers

To understand the fundamental basis for the pH dependent gold adsorption behavior of DELT to gold and its optimum near pH 7.0, we carried out solution titration experiments on the monomers DELT, as well as DEDT and L-tyrosine. We were forced to perform the titration experiments on monomers and not polymerized DELT since the HRP polymerization products were not sufficiently soluble in aqueous solution to carry out homogeneous aqueous phase titrations. We performed the titrations starting at around pH 3.0 and went to successively higher pH values with the addition of small constant aliquots of base until we covered the pH range from 3–11. Since the data were not obtained under CO_2 free conditions, in the range around 7–8 equilibrium pH values could not be determined sufficiently rapidly because of the minor carbonate equilibrium slowly changing the pH. Therefore, these values are not shown. However, the molarity of H^+ consumed in this region due to the carbonate equilibrium is small, assuming CO_2 saturation of the solution, with respect to the molarity of monomers being titrated. Therefore, no significant consumption of H^+ is evident in this pH region compared to the monomer titration regions, which dominate the titration curve. The titration results are presented in Figure 4 as the normalized quantity, H^+ moles/n, the moles H^+ consumed per n moles of the monomer, plotted vs. the pH value at each given point in the titration. This presentation makes clear that the DELT and DEDT isomers behave identically, within experimental error, but they clearly behave differently from that of L-tyrosine.

The titration differences between DELT and L-tyrosine can account for the gold adsorption properties of polymerized DELT that we measured and the relative solubility of polymerized L-tyrosine. Deprotonation changes in the chemical structure of DELT and L-tyrosine with increasing pH are shown in Schemes 1 and 2, respectively.

At the very lowest pH values, below that where we obtained data, the DELT, DEDT and L-tyrosine monomers all possess protonated α-NH_3^+ groups. As the pH increases, the next change in L-tyrosine corresponds to the loss of the carboxylic acid proton at low pH (pKa = 2.2), resulting in formation of the -COO^- anion and an overall zwitterion form. In Figure 4, we observe the remnant of this L-tyrosine carboxylic proton's titration as the pH is increased above 3.0. DELT and DEDT both lack this free carboxylic acid group due to their esterification by the decyl group. Consequently, they exhibit no evidence of this titration and are both net positively charged in this pH region due to the α-NH_3^+. Between pH 6 to 7, both DELT and DEDT exhibit titration behavior that is complete by pH 7.0. This is the titration due to deprotonation of the α-NH_3^+ group and results in both DELT and DEDT becoming neutral species and

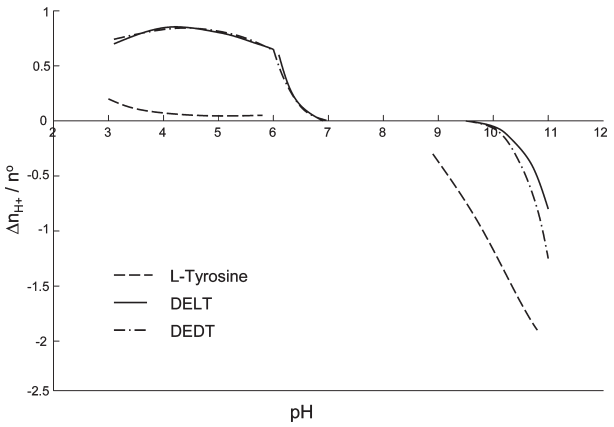

Fig. 4. Titration curves of the L-Tyrosine, DELT and DEDT monomers presented as the ratio of moles H^+ consumed/mole monomer as the pH is increased with added NaOH.

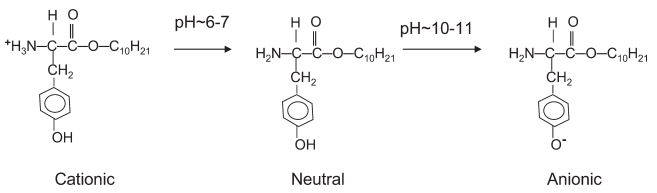

Sch. 1. DELT species involved in all pH titration transitions.

overall less hydrophilic. This pKa around 6.0–6.5 is shifted downward from that of the α-NH_3^+ group in L-tyrosine (pH = 9.1) since the carboxylate anion found in L-tyrosine is not present in DELT and DEDT to electrostatically stabilize the α-NH_3^+ proton to higher pH values, as it does in L-tyrosine. The DELT and DEDT monomers remain neutral species until around pH 9.3 where they begin to undergo titration behavior, largely between pH 10–11, that is charateristic of phenolic -OH deprotonation. Thus, between pH 7 to 9.3, DELT and DEDT are neutral species and would be expected to exhibit their lowest hydrophilicity. This fact is also suggested by data from other studies. For example, the contact angle of electropolymerized films of DELT exhibits its lowest values and therefore, is most hydrophilic as the pH approaches 9.0 (19). In other experiments, the pH dependent QCM gold surface mass binding (22) and c.m.c. measured values (17) for both DELT and DEDT monomers suggest that they self-assemble on the gold surface into structured aggregates to a greater extent as the solution pH increases to 7.0 and beyond. Thus, the Figure 3 pH 7.0 optimum in the gold surface coverage by DELT is exactly the behavior that is consistent with the pH titration data reported here and with the previously reported properties of these monomers.

For L-tyrosine, no significant titration occurs between pH 4 to 6. Therefore, in this pH range, L-tyrosine is a net neutral zwitterionic species. The Figure 4 titration curve exhibits proton consumption in the pH range between 8–9, until a pKa = 9.1 where the deprotonation midpoint of the α-NH_3^+ group occurs. This creates an anion, followed by the deprotonation of the phenolic -OH at a pKa = 10.9, resulting in a dianion monomer. The latter two deprotonation events produce net charge states of -1 and -2 that impart increased hydrophilic character to the monomer. Thus, L-tyrosine is charged at all pH values and is consequently quite hydrophilic as compared to the DELT and DEDT monomers. We know from a previous study that electropolymerized L-tyrosine forms relatively poorly adhering films on gold surfaces around neutral pH (19, 25). Nonetheless, DELT, DEDT and L-tyrosine were able to be electropolymerized and entrap horseradish peroxidase to form enzyme electrode biosensors that possessed the ability to sensitively detect down to 0.01 mM H_2O_2 (18). This film forming behavior of L-tyrosine at neutral pH has also been shown in the case of electrochemical polymerization of L-tyrosine to be due to the formation of soluble oxidized dimer, which does not adhere, and oxidized polymeric products that were weakly adherent to the gold electrode surface at neutral pH (26). The greater hydrophilic behavior is not surprising since the charged carboxylate anionic L-tyrosine lacks the decyl chains of DELT and DEDT. Interestingly, the surface of electropolymerized films formed from L-tyrosine exhibit a decreasing contact angle with increasing pH (19). This effect is consistent with our previous discussion of increasing hydrophilic character as the net charge on L-tyrosine increases with increasing pH.

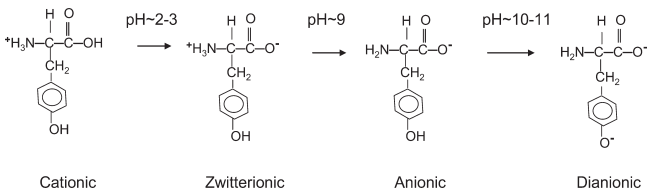

Sch. 2. L-Tyrosine species involved in all pH titration transitions.

3.4 Kinetics of Gold Coverage and Saturation by Polymerized DELT

We next determined the gold adsorption kinetic behavior of HRP polymerized DELT. Given that we observed in Figure 3 a pH 7.0 optimum for 1 h gold adsorption of polymerized DELT, consistent with the neutral charge state of this monomer at that pH determined from the titration studies, we therefore used pH 7.0 in this adsorption kinetics study. In Figure 5, following HRP polymerization of DELT for 24 h, we present the time dependent XPS data showing the increasing percentages of carbon, nitrogen and oxygen from adsorbing DELT and the decreasing gold percentage remaining on the surface. Following a rapid initial phase of DELT adsorption on the gold surface, by 20 h there is evidence of a saturation effect around 68% coverage of the surface by DELT. The 0 hr C% is 12.8%, due to adventitiously adsorbed C on the gold surface (e.g. adsorbed CO_2) prior to any DELT adsorption. Therefore, the net C% due to polymerized DELT adsorption is 68–12.7 = 55.3%. The O and N% coverages of the gold surface also achieved respective saturation values of 24.5% and 4.2%. Since the O% started at 10.3% at 0 h adsorption, due to prior strongly adsorbed CO_2, the net additional O% is 24.5–10.3 = 14.2%. The N% coverage is due entirely to adsorbed DELT, since no other N containing species is available in this experiment to adsorb to the gold surface. Therefore, this makes the O:N ratio due to the adsorbed DELT = 3.4 (14.2%/4.2%), which is in close agreement to the ratio of O:N atoms (3:1) in the adsorbed DELT monomers. However, the ratio of C/O = 55.3%/14.2% = 3.9. This is not close to the ratio of 18 C atoms to 3 O atoms = 6 in DELT. Some of this discrepancy may be accounted for on the basis of the strongly adsorbed CO_2, a species with C:O of 0.5. Fractional surface adsorption of CO_2 prior to DELT exposure, would necessarily lower the ratio observed on the surface from that expected for pure DELT.

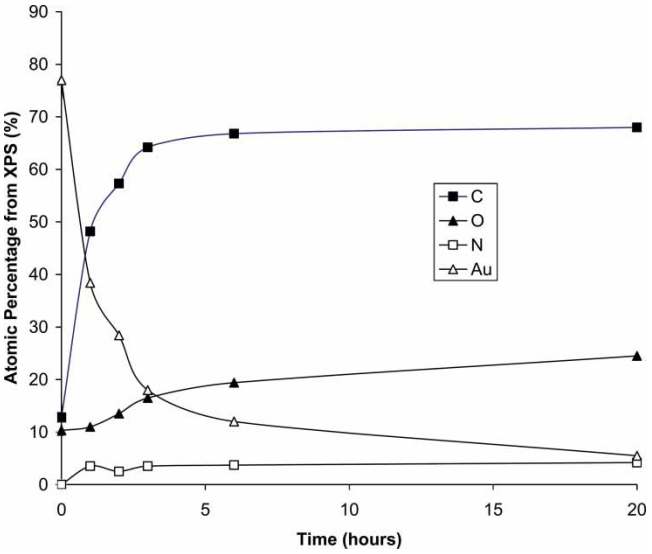

Fig. 5. Time dependent XPS measurements of DELT gold coverage by atomic %. Following a 24 h pH 6.0 polymerization by HRP, the gold substrates were immersed for the indicated times before XPS measurement.

3.5 Estimating the DELT Film Thickness

Since the XPS technique relies upon ejected electrons to reach the detector, it reveals atomic composition with exponentially decreasing sensitivity to a depth of about 10 nm from the film surface. This decreasing sensitivity can be used to estimate film thickness adsorbed to the gold substrate using Equation (1) (27).

$$I_{obs} = I_o e^{-x/\lambda} \quad (1)$$

Equation (1) represents the attenuation of the gold photoelectron intensity due to the adsorbed film, I_{obs}, relative to the unadsorbed surface gold photoelectron intensity, I_o. This attenuation level is determined by the mean free electron escape depth, $\lambda = 2.2$ nm, of MgKα excited Au4f photoelectrons with the relatively high kinetic energy 1170 eV attenuated by the overlying organic film of thickness $\times$ nm. Therefore, Equation (1) allows us to estimate the film thickness from the Au4f signal attenuation values. These methods of analyzing the XPS data mean that we can understand the atomic composition at the surface and follow the adsorption process, as well as estimate the adsorbed film thickness. In our experiments, gold has been attenuated by the film from an initial value of 77% to 5.3% effective coverage of the gold surface. We believe that this is, in fact, true saturation of the available gold surface by DELT polymer. Using Equation (1), we estimate that the polymerized DELT film possesses an average thickness of 5.89 nm. The remaining 5.3% of gold detected is due to X-ray photoelectron attenuation from the completely covered gold surface underlying the polymerized DELT film. Since these adsorption experiments were carried out below the c.m.c. in the absence of self-assembly, the possibility exists that this film thickness may correspond to successive bilayers of the DELT polymer. In such a structure, decyl chains from two different polymer strands might interact directly with each other away from the hydrophilic gold and aqueous solution environments, while the relatively hydrophilic backbones from the different strands interact with the gold surface on one side and the bulk water molecules on the other side.

4 Conclusions

Self-assembly is an important concept in materials design and this process has been documented in a wide variety of amphiphilic polymeric systems. Rod-like or tubule self-assembled aggregates, similar to those reported in other studies for the biomimetic amphiphilic monomer DELT we characterized here, have been observed in a number of small molecule amphiphilic systems (28 review). Examples include a variety of lipid structures, such as chiral ammonium amphiphiles that form helical structures (29), chiral single chain diacetylenic lipids that form ribbons and tubules under different conditions (30), and double chain diacetylenic triglyceride lipids that form hollow tubules in aqueous solution involving stacked bilayers (31).

Self-assembling systems also occur in biological polymers involving a number of prominent biological structure classes. The most important are the amphiphilic biological membrane lipid bilayer that defines the interior space of all living cells. A number of structural proteins are comprised of self-assembling polypeptides, such as collagen. Self-assembling polypeptide systems currently under study as biomimetic systems include: silk proteins (32), polypeptide molecular rods (33) and cyclic decapeptides that self-assemble into nanotubules (34), to name a few. Psuedo-poly(tyrosines), polymerized non-biologically through the phenolic -OH, have been actively studied (35). Besides good biocompatibility, these non-biological poly(amino acids) have some advantages in terms of solubility, meltability and processability.

Since the chiral DEDT and DELT species are comprised of the esterified amino acid tyrosine, they can be considered to be biomimetic monomers. The pH dependent saturation of the gold surface by adsorbing DELT polymer, polymerized below its c.m.c. value, and the 5.89 nm film thickness we observed for that DELT film, may be the result of a bilayer type of structure formed on the gold surface. As we described in the Introduction, the crosslinking and tough mechanical properties exhibited by polymeric systems comprised of phenolic monomers like these tyrosine derivatives have important biological functions in plant and marine organisms. Monomers such as DELT and DEDT may also provide biomimetic approaches to addressing various materials based problems such as providing a simple route to the electrical insulation between gold circuit lines during fabrication (36). Therefore, the pH dependent gold surface adsorption kinetic and saturation behavior we characterized represents a first step in that direction.

5 Acknowledgments

The authors wish to acknowledge the use of instrumentation within the Center for Advanced Materials at University of Massachusetts Lowell and the generous help and advice of Professor James Whitten. Also, funding is gratefully acknowledged from a TURI Grant at University of Massachusetts Lowell.

6 References

1. Dunford, B.H. In *Horseradish Peroxidase: Structure and Kinetic Properties. Peroxidases in Chemistry and Biology II*. Everse, J., Everse, K.E. and Grisham, M.B. (eds.); CRC Press: Boca Raton, FL., 1–35, 1990.
2. Colonna, S., Gaggero, N., Richelmi, C. and Pasta, P. (1999) *Trends in Biotechnology*, **17**, 163–169.
3. Dordick, J.S., Marletta, M.A. and Klibanov, A.M. (1987) *Biotechnology and Bioengineering*, **30**, 31–36.
4. Ryu, K., Stafford, D.R. and Dordick, J.S. (1989) *ACS Symp. Ser.*, **389**, 141–143.
5. Akkara, J.A., Senecal, K.J. and Kaplan, D.L. (1991) *J. Polymer Sci.*, **29**, 1561–1574.
6. Ryu, K. and Dordick, J.S. (1992) *Biochemistry*, **31**, 2588–2598.
7. Uyama, H., Kurioka, H., Kaneko, I. and Kobayashi, S. (1994) *Macromol. Rapid Commun.*, **15**, 507–512.
8. Akkara, J.A., Ayyagari, M., Bruno, F.F., Samuelson, L.A., John, V.T., Karayigitoglu, C., Tripathy, S.K., Marx, K.A., Rao, D.V.G.L.N. and Kaplan, D.L. (1994) *Biomimetics*, **4**, 331–339.
9. Ayyagari, M., Marx, K.A., Tripathy, S.K., Akkara, J.A. and Kaplan, D.L. (1995) *Macromolecules*, **28**, 5192–5297.
10. Bruno, F.F., Akkara, J.A., Samuelson, L.A., Kaplan, D.L., Mandal, B.K., Marx, K.A., Kumar, J. and Tripathy, S.K. (1995) *Langmuir*, **11**, 889–893.
11. Sarma, R., Alva, K.S., Marx, K.A., Tripathy, S.K., Akkara, J.A. and Kaplan, D.L. (1996) *Materials Science & Engineering*, **C4**, 189–192.
12. Alva, K.S., Sarma, R., Marx, K.A., Kumar, J. and Tripathy, S.K. (1997) *SPIE Smart Materials Technologies*, **3040**, 200–210.
13. Alva, K.S., Marx, K.A., Kumar, J. and Tripathy, S. (1997) *Macromolecular Rapid Communications*, **18**, 133–137.
14. Berglin, M., Delage, L., Potin, P., Vilter, H. and Elwing, H. (2004) *Biomacromolecules*, **5**, 2376–2383.
15. Lehn, J.M. (2004) *Reports on Progress in Physics*, **67**, 249–261.
16. Albrecht, M. (2007) *Naturwissenschaften*, **94**, 951–963.
17. Marx, K.A., Alva, K.S. and Sarma, R. (2000) *Materials Sci. & Eng.*, **C11**, 155–163.
18. Long, D.D., Marx, K.A. and Zhou, T. (2001) *J. Electroanal. Chem.*, **501**, 107–113.
19. Marx, K.A., Zhou, T. and Long, D.D. (2005) *Biomacromolecules*, **6**, 1698–1706.
20. Marx, K.A. *The Quartz Crystal Microbalance and the Electrochemical QCM: Applications to Studies of Thin Polymer Films, Electron Transfer Systems, Biological Macromolecules, Cells and Biosensors*; Janshoff, A. and Steinem, C. (eds.); Piezoelectric Sensors 5, Series on Chemical Sensors and Biosensors, Springer-Verlag: Berlin, 371–424, 2007.
21. Marx, K.A. *Toward Understanding the Intelligent Properties of Biological Macromolecules-Implications for Their Design into Biosensors*; Smart Biosensor Technology, Knopf, G. and Bassi, A. (eds.); CRC Press, Taylor & Francis: New York, 3–81, 2007.
22. Marx, K.A., Zhou, T. and Sarma, R. (1999) *Biotechnology Progress*, **15**, 522–528.
23. Marx, K.A. (2003) *Biomacromolecules*, **4**, 1099–1120.
24. Marx, K.A., Lee, J.S. and Sung, C. (2004) *Biomacromolecules*, **5**, 1869–1876.
25. Marx, K.A. and Zhou, T. (2002) *J. Electroanal. Chem.*, **521**, 53–60.
26. Malfoy, B. and Reynaud, J.A. (1980) *J. Electroanal. Chem.*, **114**, 213–223.
27. Hernandez, J.E., Ahn, H. and Whitten, J.E. (2001) *J. Phys. Chem. B*, **105**, 8339–8344.
28. Fendler, J.H. *Membrane-Mimetic Approach to Advanced Materials; Advances in Polymer Science*; Springer Verlag: Heidelberg; Vol. 113, 62–64, 1994.
29. Kunitake, T. and Yamada, N. (1986) *J. Chem. Soc. Chem. Commun.*, 655–663.
30. Schnur, J.M., Ratna, B.R., Selinger, J.V., Singh, A., Jyothi, G. and Easwaran, K.R.K. (1994) *Science*, **264**, 945–947.
31. Lu, M.H., Lando, J.B., Mann, J.A., Petschek, R.G. and Rosenblatt, C. (1991) *Langmuir*, **7**, 1988–1996.
32. Kaplan, D.L., Fossey, S., Viney, C. and Muller, W. *Self-Organization (Assembly) in Biosynthesis of Silk Fibers-A Hierarchical Problem*; Aksay, I., Baer, Sarikaya and Tirrell, D.A. (eds.); Materials Research Society: Pittsburgh, Vol. 255, 19–30, 1992.
33. Zhang, G., Fournier, M., Mason, T.L. and Tirrell, D.A. *Toward Monodisperse Poly(Gamma-Benzyl Alpha, L-Glutamate): Uniform, Polar, Molecular Rods*; Aksay, I., Baer, Sarikaya and Tirrell, D.A. (eds.); Materials Research Society: Pittsburgh Vol. 255, 405–410, 1992.
34. Thies, M. and Paradies, H. *Self-Assembly of Tyrocidines in Nanotubular Structures*; Mulder, Schmidt and Vogel (eds.); Materials Research Society: Pittsburgh; Vol. 489, 145–152, 1998.
35. Kohn, J. (1993) *Trends Polym. Sci.*, **1**, 206–212.
36. Angelopoulos, A., Marx, K.A. and Oh, S. *The Use of Aqueous Enzymatic Polymerization of Amphiphilic Alkyl Tyrosine Derivatives as Environmentally Benign Coatings in the Microelectronics Industry. In proceedings MRS: Polymer Interfaces and Thin Films*; Karim, A., Russell, T.P., Frank, C.W., and Nealey, P.F. (eds.); Materials Research Society: Pittsburgh, Vol. 710, 207–212, 2002.